EFDA–JET–PR(12)29

Yu.N. Dnestrovskij, S.V. Cherkasov,A.V. Danilov, A.Yu. Dnestrovskij,
S.E. Lysenko, I.A. Voitsekhovich and JET EFDA contributors

The Influence of Toroidal Rotation on Global Confinement in JET H-mode Plasmas with Different Heat Mix

The Influence of Toroidal Rotation on Global Confinement in JET H-mode Plasmas with Different Heat Mix

Yu.N. Dnestrovskij[1], S.V. Cherkasov[1], A.V. Danilov[1], A.Yu. Dnestrovskij[1], S.E. Lysenko[1], I.A. Voitsekhovich[2] and JET EFDA contributors*

JET-EFDA, Culham Science Centre, OX14 3DB, Abingdon, UK

[1]NRC 'Kurchatov Institute', Tokamak Physics Institute, Moscow 123182, Russia
[2]EURATOM-CCFE Fusion Association, Culham Science Centre, OX14 3DB, Abingdon, OXON, UK
** See annex of F. Romanelli et al, "Overview of JET Results", (24th IAEA Fusion Energy Conference, San Diego, USA (2012)).*

Preprint of Paper to be submitted for publication in
Plasma Physics and Controlled Fusion

ABSTRACT

It is known that the change of toroidal rotation velocity in JET H-mode shots strongly changes the stiffness of the ion temperature profile, but weakly influences a global confinement. The quantitative estimates of these effects are found for several selected H-mode discharges with various heat mix of combined NBI and ICRH heating. With the change of rotation velocity by factor 3, the energy confinement time changes approximately by 10%, but the stiffness of the ion temperature profile changes in the gradient zone approximately by 3 times.

1. INTRODUCTION

The dependence of the tokamak energy confinement on the toroidal rotation for plasma without internal transport barriers (ITB) was considered in [1, 2]. It was confirmed that for the ELMy H-mode JET shots the change of the toroidal rotation velocity by several times does not lead to the noticeable change of the energy confinement time τ_E [2]. At the same time, it was shown in [3] that the decrease of rotation velocity leads to the large increase of the ion temperature profile stiffness, κ_i, in the part of the plasma cross section, where the magnetic shear $s = \rho/q\ dq/d\rho$ is low enough. In the presented paper we consider these two features in more details by the analysis of several JET ELMy H-mode shots and applying as a tool the canonical profiles transport model (CPTM) [4, 5]. In Section 2 we analyze two pairs of the JET shots with high and low rotation velocities and approximately equal deposited powers to estimate the correlation between the energy confinement and rotation. In Section 3 we provide the energy balance calculations using the CPTM for chosen JET shots. In this model the heat fluxes have the structure of fluxes with critical gradients. The calculations confirm the weak correlation between κ_i and τ_E. for selected discharges. The quantitative estimates of the ion temperature profile stiffness variation in the plasma core and in the gradient zone due to change of rotation velocity are considered in Section 4. The other set of two shots with NBI and mixed heating is analyzed in Section 5. The conclusions are summarized in Section 6.

2. ANALYSIS OF THE GLOBAL ENERGY BALANCE OF JET SHOTS WITH DIFFERENT ROTATION VELOCITIES

To clarify the effect of toroidal rotation on the global confinement the analysis of four JET ELMy H-mode shots with mixed NBI and ICRH heating has been performed. For the first pair (##50624, 50628) the absorbed NBI power P_{NB} was higher than the absorbed ICRH power P_{IC} ($P_{NB} > P_{IC}$). For the other pair (##52097, 52098) on the contrary, $P_{NB} < P_{IC}$, but for all the shots the total power $P_{NB} + P_{IC}$ was approximately the same. In the first pair the toroidal rotation velocity is three times higher than in the second pair (figure 1).

We used data from the TRANSP code as the experimental data. The analysis was provided for the steady state phase of the discharges during the time interval $8 < t < 9$s. For all shots the plasma geometry and the main plasma parameters were the same:

$$R = 2.92\text{m},\ a = 0.95\text{m},\ B_0 = 2.85\text{T},\ I = 2.8\text{MA}. \qquad (1)$$

In Table 1 some other parameters are presented. Here n is the line averaged density, P_{NB} and P_{IC} are the corresponding absorbed powers averaged over the time interval $8 < t < 9$ s. The RMS errors are calculated as deviations from average values. They reflect in main the nonstationarity of scenario rather the experimental errors as we use smoothed TRANSP data. Here also $P_{tot} = P_{NB} + P_{IC} + P_{OH} - P_{rad}$, $\tau_E = W/((P_{tot} - dW/dt)$, W is the thermal energy storage and ω is the central angular frequency of toroidal rotation.

It is seen that for the first pair with high rotation velocity the values of the energy confinement time τ_E are considerably higher than for the second pair. It seems at the first glance that it is the consequence of high rotation velocity for the first pair. Nevertheless, the situation is not so simple, as the plasma densities and the values of P_{tot} are different, and these parameters govern the energy confinement.

To estimate the effect of density and power changes on τ_E we start from two pairs of shots with equal rotation velocities. We introduce the following parameters for the pairs (50624/50628) and (52097/52098):

$$\begin{aligned} &\delta n = \Delta n/n, \qquad \delta P = \Delta P/P, \qquad \delta\tau_E = \Delta\tau_E/\tau_E \\ &\Delta n = n(50624) - n(50628),\ \Delta P = P_{tot}(50624) - P_{tot}(50628), \\ &\Delta\tau_E = \tau_E(50624) - \tau_E(50628) \end{aligned} \qquad (2)$$

$$\begin{aligned} &n = \tfrac{1}{2}(n(50624) + n(50628)),\ P = \tfrac{1}{2}(P_{tot}(50624) + P_{tot}(50628)), \\ &\tau_E = \tfrac{1}{2}(\tau_E(50624) + \tau_E(50628)) \end{aligned} \qquad (3)$$

Here are the formulae for the first pair. The similar formulae are true for the second pair. We use further for density n, total power P_{tot} and energy confinement time τ_E the experimental arrays from the time interval $8 < t < 9$ s. It allows us to calculate both the averaged in time values and RMS deviations. The averaged values corresponding to (2) and (3) are shown in Table 2. In the first pair, the density in the second shot is higher, but the power is lower (see Table 1). In accordance with ITER98(y, 2) scaling [6], both factors lead to the confinement improvement, and this is consistent with data from Table 1. Lower line of Table 2 contains the pair of shots (52097/52098) with low rotation velocity. In this pair the sign of δn is opposite to the previous one, while the sign of δP is the same. This peculiarity is important for the reliability of further calculations.

As the parameters of all four shots are not far from each other, we represent the dependence of τ_E on parameters as usual scaling

$$\tau_E = \text{Const}\ n^A\ P_{tot}^{\ B}\ F(\omega_{tor}), \qquad (4)$$

where $F(\omega_{tor})$ is any function on toroidal rotation velocity. In this case

$$\delta\tau_E = A\ \delta n + B\ \delta P + \delta\tau_\omega, \tag{5}$$

where $\delta\tau_\omega = \Delta F/F$ is the change of τ_E due to rotation velocity modification.

For pairs (50624/50628) and (52097/52098) the rotation velocities are the same, therefore $\Delta F = 0$, $\delta\tau_\omega = 0$, and we obtain from the expression (5)

$$\delta\tau_E = A\ \delta n + B\ \delta P \tag{6}$$

Substituting data from Table 2 into (6), we obtain the linear set of equations relatively A and B

$$\begin{aligned} -12.6 &= -51\ A + 9.8\ B, \\ -6 &= 27\ A + 17\ B \end{aligned} \tag{7}$$

We denote the elements of the right hand part matrix through $\mathbf{a}_{ij}$. The set (7) is well defined because the ratio $\langle \mathbf{a}_{ij} \rangle / (\det \mathbf{a}_{ij})^{1/2} \sim 1$. Therefore, the errors of the solution are of the same order as the errors of the coefficients $\mathbf{a}_{ij}$. We obtain from the set (7)

$$A = 0.13 \pm 44\%, \qquad B = -0.58 \pm 24\% \qquad \tau_E \sim n^{0.13}\ P_{tot}^{\ -0.58} \tag{8}$$

The scaling (8) does not contradict to the well known ITER98(y,2) scaling [6] ($A_{y2} = 0.23$, $B_{y2} = -0.69$) and to one-machine JET scaling [7] ($A_{JET} = 0.41$, $B_{JET} = -0.4$).

Now we can compare the pairs with different toroidal rotation velocities and find the effect of the influence of these velocities on τ_E. To do this we have to return to the expression (5). In Table 3 averaged data and deviations for the pairs (50624/52098) and (50628/52097) are included and the expression $\delta\tau_\omega = \delta\tau_E - (A\ \delta n + B\ \delta P)$ is used.

We see from Tables 1–3 that the increase of the rotation velocity in 3 times leads to the increase of τ_E in the value of order 8%. It is surprising that the estimates for $\delta\tau_\omega$ in Table 3 are close one to another for both independent pairs. The error bars are large, but it is the consequence of non steady state behaviour of the input data and very uncertain calculations of dW/dt.

Summarizing, the toroidal rotation of plasma weakly affects the global energy confinement of the considered ELMy H-mode shots without internal transport barriers. This conclusion coincides qualitatively with the conclusion obtained in [2] but contains also the quantitative estimations of $\delta\tau_\omega$ presented in Table 3.

3. THE LOCAL CHANGE OF THE ION TEMPERATURE PROFILE STIFFNESS AT THE TOROIDAL ROTATION

It was concluded from experiment [3] that the ion temperature profile stiffness $\kappa_i = n\chi_i$ diminishes at the increase of the toroidal rotation velocity. This reduction is observed in the region of the

plasma core, where the magnetic shear s is low or negative. Outside this region the profile stiffness is not changed by [3] even at very high rotation velocity. In the JET experiment the change of rotation velocity was produced by the modification of the proportion between the powers of the NBI and ICRH heating. At the increase of the rotation velocity in a factor of 3 the stiffness in the plasma core decreases approximately by an order of magnitude [3]

The question arises, how can we match such a large change of the ion temperature profile stiffness with low modification of the energy confinement time τ_E reported in [2] and confirmed in the previous Section? To answer this question, we have to discuss the concept of the ion temperature profile stiffness. We remind at first the main points of the transport models with critical gradients based on the idea of the profile stiffness [4, 8]. The heat fluxes q_α in the electron and ion channels ($\alpha = e, i$) are as follows:

$$q_\alpha = -\kappa_\alpha T_\alpha (T_\alpha'/T_\alpha - g_\alpha) H(-[T_\alpha'/T_\alpha - g_\alpha]) - n\chi_\alpha^0 T_\alpha' + 3/2\, \Gamma T_\alpha \quad (9)$$

where κ_α is the stiffness, g_α is the critical gradient, $T_\alpha' = \partial T_\alpha/\partial\rho$, $H(x)$ is a Heaviside function, Γ is the particle flux and χ_α^0 is the heat diffusivity due to processes not connected with critical gradients (e.g. neoclassical). In our model of canonical profile [8, 9]

$$g_\alpha = g_\alpha(\rho) = T_c'/T_c \quad (10)$$

$$\kappa_\alpha = C_{T\alpha} (1/M) (a/R)^{0.75} q(\rho = \rho_{max}/2) q_{cyl} (T_\alpha(\rho = \rho_{max}/4))^{1/2} (3/R)^{1/4} (1/B_0) \bar{n} = \text{const}(\rho) \quad (11)$$

where T_c is the canonical profile of temperature, which independent on type of particles (electrons or ions), $C_{Te} = 3.5$, $C_{Ti} = 5$, B_0 is the toroidal magnetic field at the magnetic axis in Tesla, T_α in keV, a and R in m. The coefficient κ_α was obtained on the basis of NBI shots with high rotation velocities [10].

The degree of profile stiffness is defined by a dimensionless parameter K which in practical units is as follows

$$K = \kappa T/(625\, a^2 Q), \quad (12)$$

where κ is the profile stiffness in 10^{19} $m^{-1}s^{-1}$, T is the characteristic temperature in keV, Q is the characteristic density of the deposited power in MW/m^3. The temperature profile is stiff, if

$$K > 1 \quad (13)$$

In this case the relative gradient T_α'/T_α is close to the critical gradient g_α and the difference ($T_\alpha'/T_\alpha - g_\alpha$) is small, therefore, the high changes of κ_α lead to low changes of the temperature profile.

To verify quantitatively these considerations we provide transport calculations using the following auxiliary model. We introduce the artificial stiffness function

$$S(\rho,\rho_0) = S_0 \ (0 < \rho < \rho_0), \qquad S(\rho,\rho_0) = S_1 \ (\rho_0 < \rho < \rho_{max}) \tag{14}$$

and use the product $S\,\kappa_i$ in the ion heat flux ($\alpha = i$) (9) instead of κ_i. The electron heat flux ($\alpha = e$) remains as previously. The value of S defines the change of stiffness in the ion channel.

We put at first

$$\rho_0 = \rho_{max} \tag{15}$$

and provide transport calculations for the shot #52097 (ICRH dominated) with several values of S_0 (the value S_1 is absent in the model (15)). Figure 2 presents the ion temperature profiles calculated by the model (14)-(15) for S_0 = 0.2, 1, 2, 5 and 10. The values of pedestals are calculated by the nonlinear CPTM model [5]. The experimental ion temperature profile is also plotted. One can mention that at S_0 = 1 the calculated ion temperature is slightly higher than the experimental one. It is happened as the stiffness of the model was found in [10] for NBI shots only with high rotation velocities. The temperature profile at S_0 = 2 is more close to experiment in the gradient zone $0.5 < \rho < 0.8\ \rho_{max}$. This feature hints at the increase of stiffness due to the decrease of rotation velocity as the velocity in the shot #52097 is low. At further increase of the stiffness S_0, the calculated temperature diminishes rather slowly.

The profiles of the ratio $R/L_{Ti} = -\,R\,T_i'/T_i$ at S_0 = 1, 2, 5 and 10 for the model (15) are presented in figure 3. The behaviour of the dimensionless critical gradient $-Rg_i = -\,R\,T_c'/T_c$ is also plotted. At S_0 = 1 the difference $R/L_{Ti} - R/L_c$ is high enough as $K \sim 0.5$. It is seen from figure 3 that this difference at the transition from S_0 = 1 to S_0 = 10 diminishes (at the point $\rho = 0.5\ \rho_{max}$) approximately in a factor of 3 instead of 10. It is due to the increase of ion heat flux for account of electrons and the corresponding increase of Q in (12). Therefore the value of K is not proportional to S_0 in these calculations.

Now we put

$$\rho_0 = 0.5\ \rho_{max} \tag{16}$$

and repeat the calculations. The profiles of the ion temperature for the same values of S_0 and S_1 = 1 are presented in figure 4. Figure 5 presents the profiles of normalized gradients of ion temperature at different stiffness factors S_0 and S_1 = 1. It is seen that in the case (16) all changes practically take place in the internal region $\rho < 0.5\ \rho_{max}$.

We can compare the results obtained by the models (15) and (16). The dependencies of the ratio $T_{i0}(S_0) / T_{i0}(S_0 = 1)$ on the parameter S_0 for both models are presented in figure 6. It is seen that

the increase of the stiffness by a factor of 10 over the whole of plasma cross section (model (15)) diminishes the central temperature down to 40%. The similar increase of the stiffness by 10 times in the plasma core (model (16)) diminishes the central ion temperature by 20% only.

The dependence of normalized energy confinement time $\tau_E(S_0) / \tau_E(S_0 = 1)$ on the parameter S_0 is presented in figure 7. For the model (15) the increase of stiffness in 10 times diminishes τ_E down to 20%. But for the model (16) the decrease of τ_E at the transition from $S_0 = 1$ to $S_0 = 10$ (at $S_1 = 1$) is on the level of 2%. Such small changes could not be reliably detected in experiment.

4. DISCUSSION

We consider now two questions:

(a) Is the stiffness of ion temperature profile constant over the plasma radius?

(b) In what manner the stiffness changes with the change of rotation velocity?

(a) It was assumed in our transport model (11) that stiffness κ_i is constant over the plasma radius. But the analysis of JET experiments [3] has shown that the stiffness in the gradient zone is higher than in the plasma core. Figure 2, calculated by the model (15), confirms such a conclusion. It is seen that at $S_0 = 1$ the $T_i(\rho)$ profile is close to the experimental one $T_i^{exp}(\rho)$ in the plasma core and notably differs from it in the gradient zone. The situation is opposite in the case $S_0 = 2$: the $T_i(\rho)$ profile is close to $T_i^{exp}(\rho)$ in the gradient zone and differs in the plasma core. It appears from this that adopted model (15) is not adequate to experiment and the model (16) at $S_0 < S_1$ is more correct.
(b) It was found in [3] that the increase of rotation velocity in a factor of 3 leads to the decrease of the stiffness in plasma core in approximately 10 times. The change of stiffness in the gradient zone due to the change of rotation velocity was not observed.

Now we analyze our results. In agreement with figure 7, if stiffness changes in 10 times in the plasma core and is not modified in the gradient zone then the change of the energy confinement time $\delta\tau_E$ is not higher than 2%. However, the analysis of the experimental data performed in Section 2, provided the estimation $\delta\tau_E \sim 8 – 10$ % due to rotation change. The same estimation was found in [2]. Therefore, the stiffness in the gradient zone has to be modified also, if the rotation velocity changes. It is possible to estimate the value of the stiffness change in the gradient zone with the help of the same figure 7, using the curve calculated by model (15). We see that the estimation $\delta\tau_E \sim 10\%$ corresponds to $S_0 = 2–3$. Figure 8 presents the comparison of calculated ion temperature profiles $T_i(\rho)$ for JET Pulse No: 52097 with dominated ICRH heating and Pulse No: 50628 with dominated NBI heating. We used for calculations the model (16) with $S_0 = 0.6$, $S_1 = 2$ for shot #52097, and $S_0 = 0.3$, $S_1 = 1$ for Pulse No: 50628. It is seen that the calculation results reasonably meet experiment. Underline that the stiffness of $T_i(\rho)$ profile in the gradient zone for the shot with low rotation velocity exceeds two times the stiffness in the shot with high rotation velocity. The same stiffness increase we obtained from the estimation of $\delta\tau_E$. The ratio S_1/S_0 (the ratio of stiffness in the gradient zone to stiffness in the plasma core) is close to 3 for both cases of shots with high and low rotation velocity.

5. THE MODELING OF JET PULSE NO'S 78032 AND 78065

To verify the results of previous sections we carried out the modeling of two JET shots from recent series discussed in [2]. The first shot #78032 had the NBI heating only with power of P_{tot} ≈14.8MW and high angular toroidal rotation velocity $\omega \sim 8\times10^4$ rad/sec. The second Pulse No: 78065 had mixed NBI and ICRH heating with approximately the same total power $P_{tot} \approx 14.9$MW and lower rotation velocity $\omega \sim 3.4\times10^4$ rad/sec. The plasma densities were also close to each other: $n \sim 5.6\times 10^{19}$ m^{-3} in the first shot, and $n \sim 5.35\times10^{19}$ m^{-3} in the second one. The other main plasma parameters were identical: the plasma current $I = 2.5$MA, the toroidal magnetic field $B = 2.7$T, the minor radius $a = 0.96$ m, the elongation $k = 1.67$ and the triangularity $\delta = 0.26$. The full nonlinear CPTM was used for the modeling [5, 9], and the model parameters were equal for both shots. We supposed for simplicity that the stiffness of the temperature profiles did not depend on radius which corresponds to (15) of $S_0 = 1$.

In the figure 9 (a,b) one can see the calculated and experimental temperature profiles of ions (a) and electrons (b) for the Pulse No: 78032 with pure NBI heating at the steady state stage of the discharge at the moment $t = 13$ sec. The NBI powers deposited to ions and electrons were equal to $P_{NBi} = 9.6$MW and $P_{NBe} = 4.9$MW correspondingly and the radiation power was $P_{rad} = 4.3$MW. The profiles of the calculated effective heat diffusivities for ions χ_i^{eff} and electrons χ_e^{eff} are shown in the figure 10. It is seen that in the gradient zone the ratio $\chi_i^{eff} / \chi_e^{eff}$ equals to 8 approximately. It is seen also that the CPTM describes reasonably the profiles of the ion and electron temperatures in the shot with pure NBI heating. The RMS deviations will be discussed further.

We consider now the modeling results for the Pulse No: 78065 with mixed heating and lower rotation velocity. Figure 11(a,b) shows the calculated and experimental profiles of the ion (a) and electron (b) temperatures in the steady state at the time moment $t = 13$ sec with $S_0 = 1$ and $S_0 = 3$. In this case $P_{NBi} = 4.9$MW, $P_{ICi} = 2.6$MW, $P_{NBe} = 2.8$MW, $P_{ICe} = 4.6$MW with "IC" index marking the ICRH power. The profiles of the corresponding effective heat diffusivities are shown in the figure 12. It is seen that in this case also the ratio of diffusivities is high enough: $\chi_i^{eff} / \chi_e^{eff} \sim 5$. The decrease of this ratio in comparison with previous case is connected with the increase of the deposited power in the electron channel ($P_e = 4.9$MW in the Pulse No: 78032 and $P_e = 7.4$MW in the Pulse No: 78065). In spite of the stiffness increase in 3 times at the transition from $S_0 = 1$ to $S_0 = 3$ the effective heat diffusivity increases in 25% only. This is happened due to flexibility of the heat flux in the form (9).

The calculation results and their comparison with the experiment are summarized in the Table 4. Here for both considered shots one can see the RMS deviations d_2T_i and d_2T_e of the calculated ion and electron temperature profiles from the experimental ones. The values of the stiffness coefficient S_0 are also shown. The values of the effective heat diffusivities at the middle of minor radius and the values of the angular rotation velocity at the magnetic axis are also included. In the last line of Table 4 the calculation results for the initial part of the Pulse No: 78065 (at $t = 9$sec) when there was the NBI heating only are presented. It is seen from this Table that the shots with pure NBI

heating (the first and the fourth lines) are reasonably modeled by the CPTM with $S_0 = 1$. The shot with mixed heating and low rotation velocity is poorly described with $S_0 = 1$, the RMS deviation here is as high as 36%. The triple increase of S_0 (the increase of the ion temperature stiffness) decreases the deviations d_2T_i and d_2T_e in 3–4 times. The change of the electron temperature occurs due to the change of the heat flux from ions to electrons.

The modeling provided in this Section develops the results of the previous Sections. We can conclude now that the increase of the toroidal rotation velocity in 2.5 times diminishes the stiffness of the ion temperature profile in the gradient zone, determining in main the energy transport in the ion channel, in 3 times approximately.

CONCLUSION

For the JET ELMy H-mode shots without ITBs the energy confinement time τ_E weakly depends on the toroidal rotation velocity. At the change of rotation velocity in three times the value of τ_E changes by 8–10 % only. It is a consequence of two features:

(i) The change of the ion temperature stiffness over the whole plasma cross section weakly influences the energy confinement time due to the flexible structure of the heat flux: the heat flux is proportional to the product of the stiffness coefficient on the difference of the gradient and critical gradient of the ion temperature. Therefore the first plasma response to the stiffness increase is to diminish the relative gradients difference keeping the absolute values of temperature practically unchanged.

(ii) The stiffness of the ion temperature profile in the experiment depends on the toroidal rotation velocity and changes over the whole plasma cross section with the modification of rotation velocity. During the change of rotation velocity in 2.5–3 times the ion temperature stiffness in the gradient zone changes in 3 times approximately.

ACKNOWLEDGEMENTS

This work was partly carried out within the framework of the European Fusion Development Agreement Work, and partly funded by the Consultancy Agreement with UKAEA 3000167220, RCUK Energy Program under grant EP/I501045 and the European Community under the contract of Association between EURATOM and CCFE, and by Russian RFBR Grant 11-07-00567. The views and opinions expressed herein do not necessarily reflect those of the European Commission.

REFERENCES

[1]. Politzer P A *et al* 2008 *Nuclear Fusion* **48** 075001
[2]. Versloot T W *et al* 2011 *Nuclear Fusion* **51** 103033
[3]. Mantica P *et al* 2009 *Physical Review Letters* **102** 175002
[4]. Dnestrovskij Yu N, Pereverzev G V 1988 *Plasma Physics and Controlled Fusion* **30** 47
[5]. Dnestrovskij Yu N, Dnestrovskij A Yu and Lysenko S E 2005 *Plasma Physics Reports* **31** 529

[6]. Progress in ITER Physics Basis 2007 *Nuclear Fusion* **47** S109
[7]. De Vries P C *et al* 2008 *Nuclear Fusion* **48** 065006
[8]. Rebut P H, Lallia P P and Watkins M L, in Plasma Physics and Controlled Nuclear Fusion Research 1988 (Proc. 12th Int. Conf. Nice, 1988), Vol. 2, IAEA, Vienna (1989) 191
[9]. Dnestrovskij Yu N *et al* 2007 *Plasma Physics and Controlled Fusion* **49** 1477
[10]. Dnestrovskij Yu N *et al* 1995 *Nuclear Fusion* **35** 1047

Shot No	n (10^{19} m^{-3})	P_{NB} (MW)	P_{IC} (MW)	P_{tot} (MW)	τ_E (s)	Central ω_{tor} (10^4 rad/s)	Dominated heating
50624	3.21±1.4%	5.93±4.2%	4.43±1.2%	10.0±2.7%	0.36±3.5%	8.1± 6%	NBI
50628	5.4±1.2%	6.16±1.8%	3.17±8.1%	9.04±3.4%	0.41±4.1%	7.8±2%	NBI
52097	4.55±3.8%	3.85±1.8%	9.55±9.3%	13.1±5.2%	0.3±10%	2.9± 10%	ICRH
52098	3.46±3.3%	2.32±1.9%	9.15±2.3%	11.0±2.5%	0.32±5.8%	3.0±9.4%	ICRH

Table 1: Main parameters of shots under study averaged over 8-9 s with the error bars determined as a RMS deviation from the averaged value.

## shots	δn	δP	$\delta\tau_E$
50624/50628	- 0.51±1%	0.1±39%	- 0.12.6±36%
52097/52098	0.27±6%	0.17±37%	- 0.06±86%

Table 2: Pairs of shots with equal rotation velocities.

## shot	δn	δP	$\delta\tau_E$	$\delta\tau_\omega$
50624/52098	– 0.075±25%	– 0.1±23%	0.13±49%	0.082±72%
50628/52097	0.17±16%	– 0.36±13%	0.32±22%	0.08±73%

Table 3: Pairs of shots with different rotation velocities.

	shot No	t, sec	Heating	S_0	d_2T_i %	d_2T_e %	$\chi_i(0.5)$ ^{2}/sec	$\chi_e(0.5)$ m^2/sec	ω 10^4 rad/sec
1	78032	13	NBI	1	20	11	3.8	0.6	8
2	78065	13	NBI+ICRH	1	36	15	4	1	3.4
3	78065	13	NBI+ICRH	3	10	4	5	1	3.4
4	78065	9	NBI	1	14	13	4	0.5	8

Table 4: Comparison of experiment with calculations.

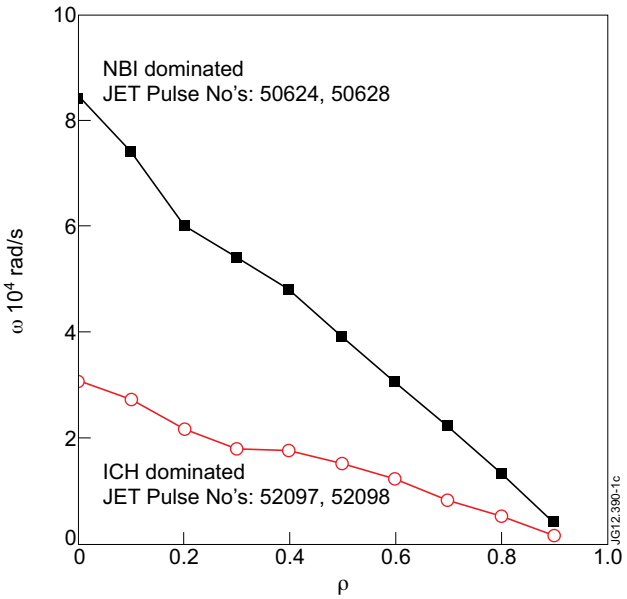

Figure 1: The typical toroidal rotation velocity profiles for the shots from Table 1.

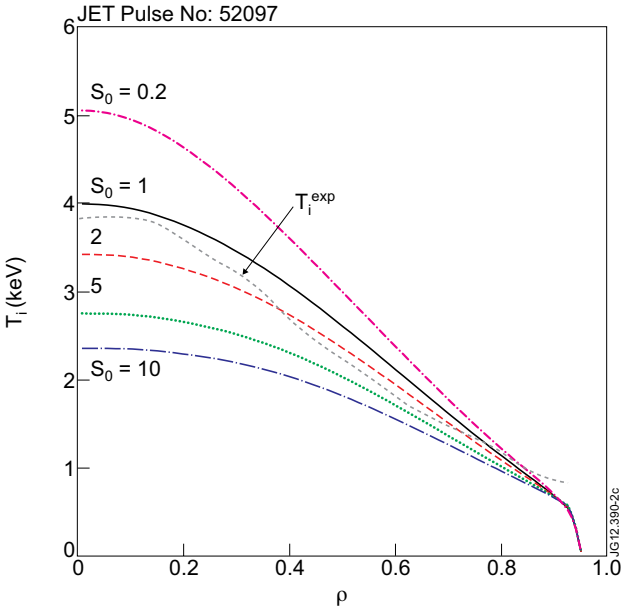

Figure 2: Model (15). Ion temperature profiles at different stiffness factors S_0 for the ICRH dominated JET Pulse No:52097, dashed line is experiment.

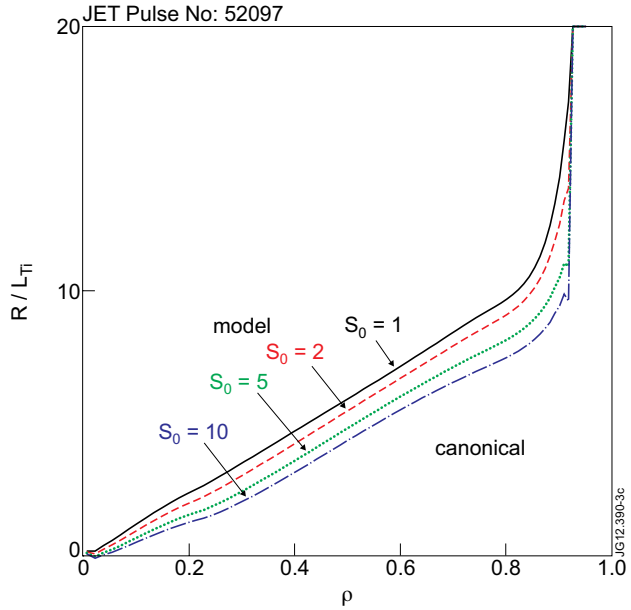

Figure 3: Model (15). Profiles of normalized gradients of ion temperature at different stiffness factors for JET Pulse No:52097.

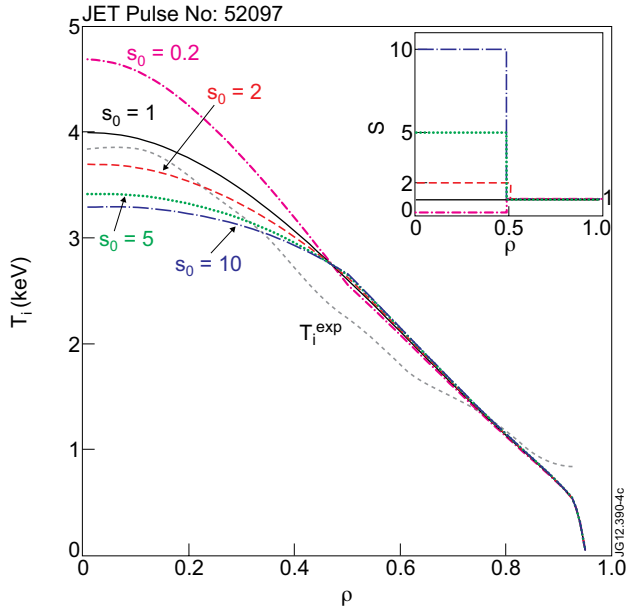

Figure 4: Model (16). Ion temperature profiles at different stiffness factors S_0 and $S_1 = 1$ for JET shot Pulse No:52097. Insertion shows profiles of stiffness factor.

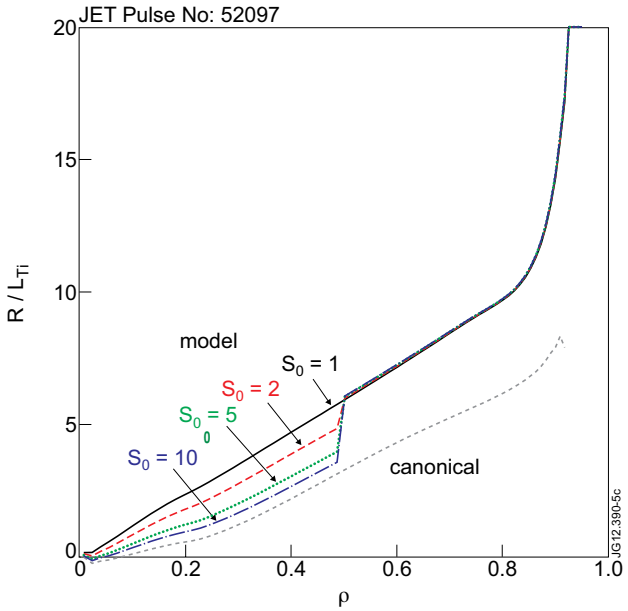

Figure 5: Model (16). Profiles of normalized gradients of ion temperature at different stiffness factors S_0 and $S_1 = 1$ for Pulse No:52097

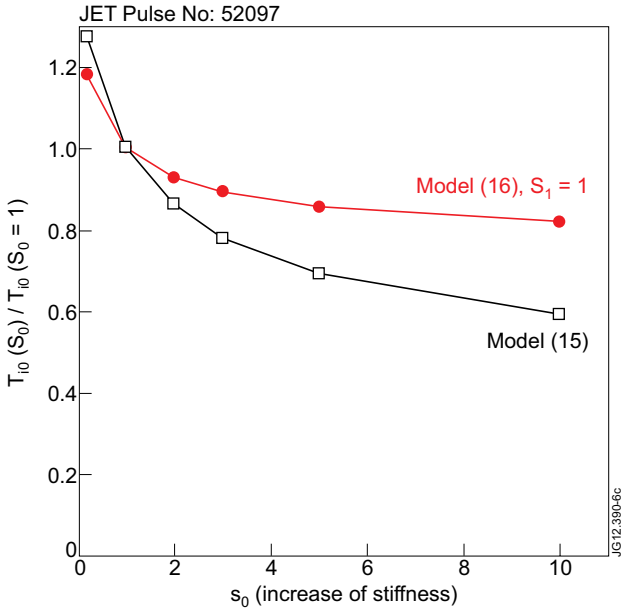

Figure 6: The dependence of the ratio $T_{i0}(S_0)$ / $T_{i0}(S_0 = 1)$ on the stiffness parameter S_0 for the models (15) and (16) (at $S_1 = 1$).

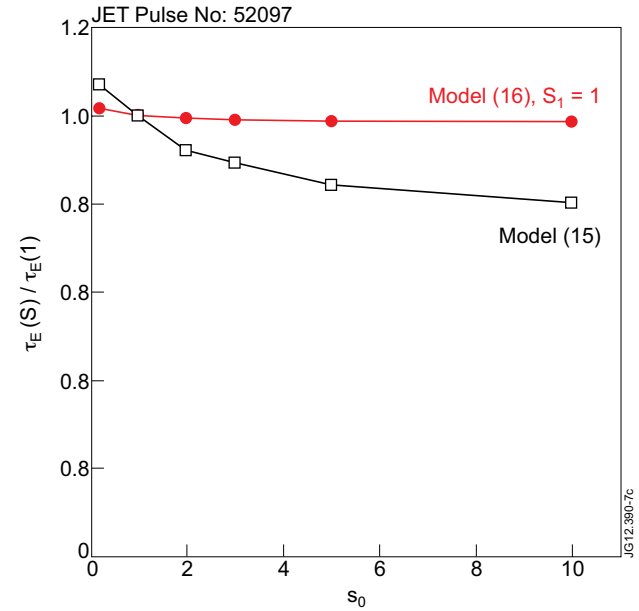

Figure 7: The dependence of the normalized energy confinement time $\tau_E(S_0)$ / $\tau_E(S_0 = 1)$ on the stiffness parameter S_0 for the models (15) and (16) (at $S_1 = 1$).

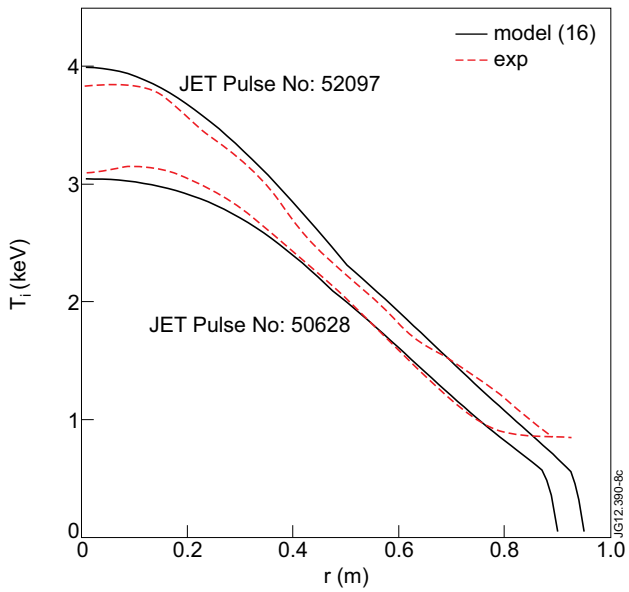

Figure 8: Profiles of ion temperature. Solid lines: calculations by the model (16) with $S_0 = 0.6$, $S_1 = 2$ for Pulse No: 52097 with low rotation velocity and with $S_0 = 0.3$, $S_1 = 1$ for Pulse No: 50628 with high rotation velocity. Dashed lines are experiments.

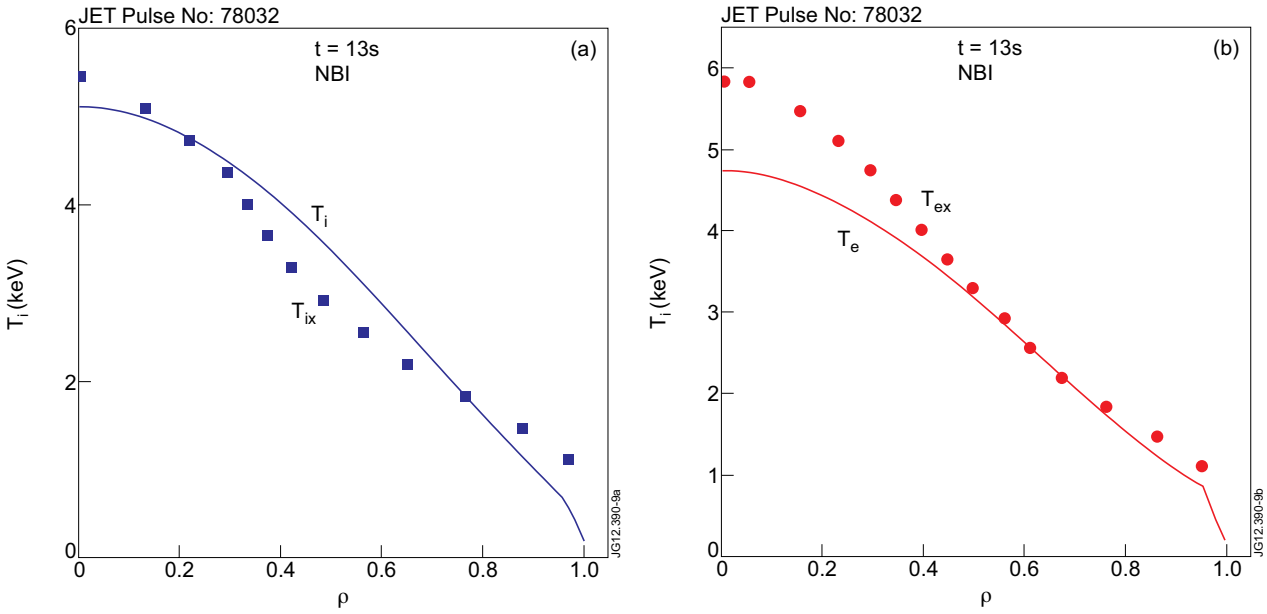

Figure 9: Calculated and experimental ion (a) and electron (b) temperature profiles for the Pulse No: 78032 with NBI heating and model stiffness parameter $S_0 = 1$.

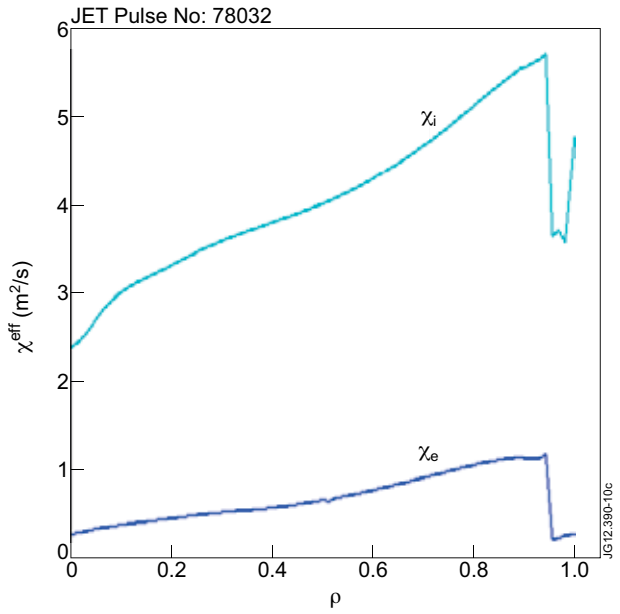

Figure 10: Calculated ion and electron effective heat diffusivity profiles, χ_i^{eff} and χ_e^{eff}, for the NBI Pulse No: 78032 at $t = 13$ sec with $S_0 = 1$.

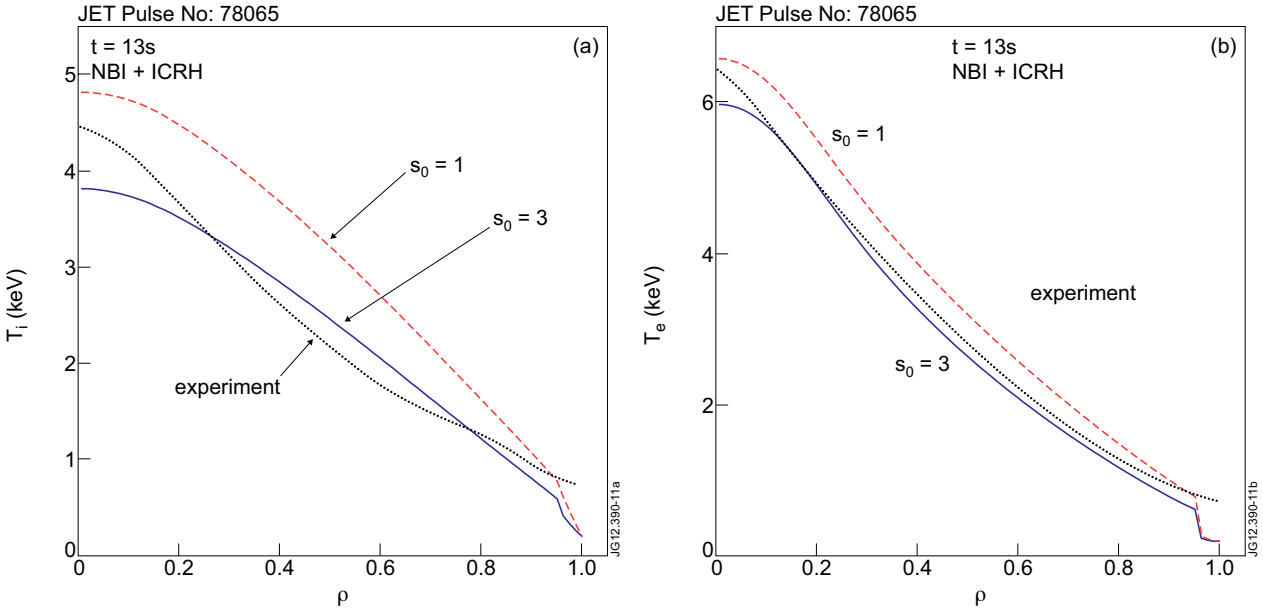

Figure 11: Calculated and experimental ion (a) and electron (b) temperature profiles for the Pulse No: 78065 with mixed heating and with stiffness parameter S_0 = 1 and 3.

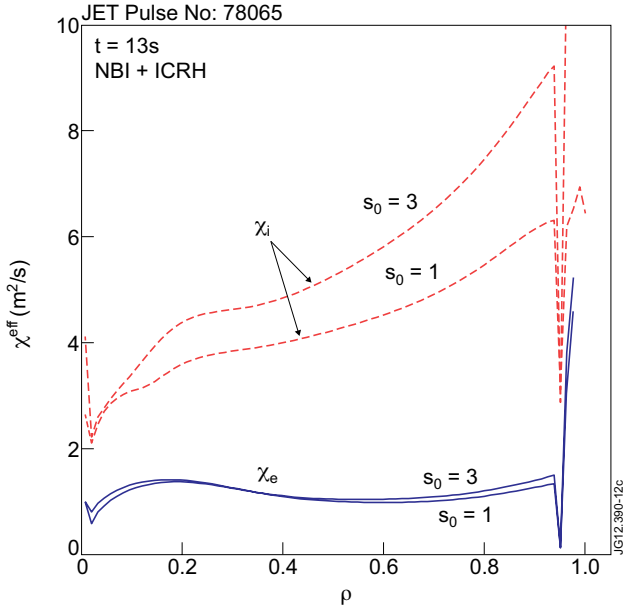

Figure 12: Calculated ion and electron effective heat diffusivity profiles, χ_i^{eff} and χ_e^{eff}, for sPulse No: 78065 at t = 13 sec with S_0 = 1 and 3.